Analysis of Spherical Shell Solutions for the Radially Symmetric Aggregation Equation

Balagué Guardia, D.; Barbaro, A.B.T.; Carrillo, Jose Antonio; Volkin, Robert

Important note
To cite this publication, please use the final published version (if applicable).
Please check the document version above.

Analysis of Spherical Shell Solutions for the Radially Symmetric Aggregation Equation[*]

Daniel Balagué Guardia[†], Alethea Barbaro[†], Jose A. Carrillo[‡], and Robert Volkin[§]

Abstract. We study distributional solutions to the radially symmetric aggregation equation for power-law potentials. We show that distributions containing spherical shells form part of a basin of attraction in the space of solutions in the sense of "shifting stability." For spherical shell initial data, we prove the exponential convergence of solutions to equilibrium and construct some explicit solutions for specific ranges of attractive power. We further explore results concerning the evolution and equilibria for initial data formed from convex combinations of spherical shells.

Key words. aggregation equation, gradient flow, spherical shells

AMS subject classifications. 35Q70, 35F25, 35Q92

DOI. 10.1137/20M1314549

1. Introduction and general problem. Agent based models have become a rich subject of study in kinetic theory. Various models have been proposed and studied regarding the collective motion of biological organisms. In this paper, we focus on a macroscopic system of nonlocal interaction equations governing biological aggregation referred to as the aggregation equation. These equations have been proposed as basic models for collective behavior, and they show up in different forms in many application areas. For instance, these equations are used to study phenomena such as insect swarms [11, 19, 34, 47, 53, 52], bird flocking [1, 37, 48, 49], schools of fish [7, 8, 13, 28], and bacteria colonies [29, 14, 15]. These models also appear in descriptions of vortex density evolution in superconductors [3, 43, 31, 45, 46, 50, 51, 57, 47, 54], self-assembly of particles [39], opinion formation [38, 35], and simplified models for granular media [23, 24, 9, 41, 55]. We refer the reader to [21, 40] for recent reviews on this subject.

We write the aggregation equation for a density of particles $\rho(t, x)$ with velocity $v(t, x)$ as

$$\frac{\partial \rho}{\partial t} + \nabla \cdot (\rho v) = 0, \qquad v = -\nabla W * \rho.$$

[†]Delft Institute of Applied Mathematics, Delft University of Technology, 2628 XE Delft, the Netherlands (danielbalague@gmail.com, A.B.T.Barbaro@tudelft.nl).
[‡]Mathematical Institute, University of Oxford, Oxford OX2 6GG, UK (carrillo@maths.ox.ac.uk).
[§]Department of Mathematics, Applied Mathematics, and Statistics, Case Western Reserve University, Cleveland, OH 44106-7058 USA (rpv17@case.edu).

The repulsive-attractive potential $W(x)$ drives the particle dynamics of the system. Particles attract each other when far apart but repel each other when very close. We restrict our attention to potentials which are radially symmetric and follow a power law, specifically,

$$W(x) = \frac{|x|^a}{a} - \frac{|x|^b}{b}, \qquad a > b > -d,$$

where d is the dimension of the space in which the particles move, typically 2 or 3. We use the standard convention that $\frac{|x|^c}{c}$ is interpreted as $\log|x|$ when $c = 0$.

Such a system has a naturally associated entropy/interaction energy. Assuming that the potential W is bounded below, we describe this interaction energy by first defining the following functional $E[\mu, \nu] \in (-\infty, \infty]$ for finite measures μ and ν on $\mathbb{R}^d$:

$$(1.1) \qquad E[\mu, \nu] = \frac{1}{2} \iint_{\mathbb{R}^d \times \mathbb{R}^d} W(x - y) \, d\mu(x) d\nu(y).$$

Using the notation that $E[\mu] = E[\mu, \mu]$, the interaction energy for the density $\rho(t, x)$ is

$$E[\rho](t) = \frac{1}{2} \iint_{\mathbb{R}^d \times \mathbb{R}^d} W(x - y) \rho(t, x) \rho(t, y) \, dx dy.$$

As established in [2, 23, 24, 56], the aggregation equation is a gradient flow of this energy functional on the space of probability measures with finite second moment $\mathcal{P}_2(\mathbb{R}^d)$ equipped with the 2-Wasserstein metric under additional assumptions on the interaction potential W. Solutions travel along paths of steepest descent, decreasing the functional until reaching a fixed point. This structure is central to the new results presented in this paper.

It has been further established in [12, 6, 5] that for radially symmetric potentials with repulsive power not worse than Newtonian, if the initial distribution is radially symmetric, compactly supported, and an element of the Sobolev space $W^{2,\infty}(\mathbb{R}^d)$, then the problem is well-posed and solutions remain radially symmetric and confined for all time. Invoking the radial symmetry and writing $\tilde{\rho}(t, r) = \omega_d r^{d-1} \rho(t, r)$, where ω_d is the surface area of the unit sphere in $\mathbb{R}^d$, the aggregation equation becomes

$$(1.2) \qquad \frac{\partial \tilde{\rho}}{\partial t} + \frac{\partial}{\partial r} (\tilde{\rho} \tilde{v}) = 0, \qquad \tilde{v}(t, r) = \int_0^\infty \omega(r, s) \tilde{\rho}(t, s) ds,$$

where

$$(1.3) \qquad \omega(r, s) = -\frac{1}{\omega_d} \int_{\partial B(0,1)} \nabla W(re_1 - s\eta) \cdot e_1 d\sigma(\eta).$$

In this notation, $\partial B(0, 1)$ is the boundary of the unit ball in $\mathbb{R}^d$ and σ is the area measure on its surface. Similarly, the energy functional can be rewritten as

$$(1.4) \qquad E[\tilde{\rho}](t) = \frac{1}{2\omega_d} \iint_{\mathbb{R}_+^2} \int_{\partial B(0,1)} W(re_1 - s\eta) \tilde{\rho}(t, r) \tilde{\rho}(t, s) \, d\sigma(\eta) dr ds.$$

Several papers exist addressing aspects of the energy minimizers. Existence results may be found in [18, 16]. In [4], it is proved that the dimensionality of the local minimizer of
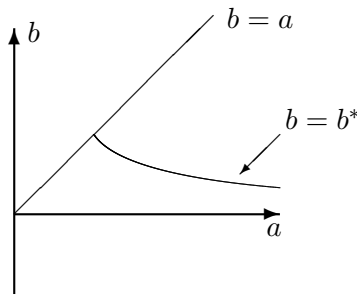
Figure 1. *Parameter regime diagram.*

the energy functional must be at least $2 - b$ for $b \in (2 - d, a)$. These geometric results are expanded upon in [20, 42]. Several stability results in radial coordinates can be found in [5]. To elaborate further, they define the following quantities dependent on a, b, and d,

$$(1.5) \qquad R_{ab} = \frac{1}{2} \left[\frac{\beta \left(\frac{b+d-1}{2}, \frac{d-1}{2} \right)}{\beta \left(\frac{a+d-1}{2}, \frac{d-1}{2} \right)} \right]^{\frac{1}{a-b}}, \qquad b^* = \frac{(3-d)a - 10 + 7d - d^2}{a + d - 3},$$

where $\beta(x, y) = \frac{\Gamma(x)\Gamma(y)}{\Gamma(x+y)}$ is the beta function. If $b \in (b^*, a)$, then the uniform distribution on the spherical shell of radius R_{ab}, denoted by $\delta_{R_{ab}}$, is a stable steady state. If $b \in (-d, b^*)$, then $\delta_{R_{ab}}$ is unstable. We present the parameter regimes in Figure 1 for clarity.

Close attention has been paid to potentials where the attractive exponent is an integer multiple of 2, i.e., $a = 2k$ for $k \in \mathbb{N}$, especially $a = 2, 4$. The authors of [22] provide a general procedure for constructing candidate explicit equilibrium solutions for even $a > 0$ and $b \in (-d, b^*)$ based on minimizing the interaction energy. We refer to these possible minimizers as the Carrillo–Huang equilibria. When $a \geq 4$, the proposed equilibria are only viable when $b \in (-d, \bar{b})$, where $\bar{b} = \frac{2+2d-d^2}{d+1} < b^*$. All of these solutions can be converted to radial form by taking $\tilde{\rho}(r) = \omega_d r^{d-1} \rho(r)$. Since we only consider the radially symmetric case, we drop all tildes from this point forward for clarity.

Uniqueness of minimizers for the case $2 \leq a \leq 4$ and $b < 0$ is addressed in [44]. The proof of uniqueness relies on strict convexity of the energy functional on an admissible set of solutions in $L^1(\mathbb{R}^d) \cap L^\infty(\mathbb{R}^d)$. Unfortunately, equilibrium solutions to the aggregation equation cannot be expected to be uniformly bounded except when the repulsive component of the potential is sufficiently singular near the origin, specifically $b \leq 2 - d$ for the Carrillo–Huang equilibria. Much of the theory for the aggregation equation involves a functional setting of L^p-spaces. This setting provides many important and deep results, such as existence and uniqueness for solutions [12] and the previously mentioned uniqueness of minimizers of the interaction energy [44]. Yet, distributional solutions also arise quite naturally. The previously mentioned steady state $\delta_{R_{ab}}$ for the PDE is one example. Another example [11] shows that in the underlying particle system solutions tend toward steady states formed from multiple spherical shells. Understanding these steady states may also help shed light on continuous ones, such as the proposed Carrillo–Huang equilibria, if the number of spherical shells tends toward infinity. In fact, based on the results in [4] about the dimensionality of the support of

the equilibria, one could conjecture that Morrey spaces of measures are a natural setting for the global well-posedness of the aggregation equation in the range of exponents $b \in (2-d, 2)$. However, this question is still widely open.

Throughout this paper, we discuss radial probability distributions that contain spherical shells. These shells correspond to a uniform distribution of particles on the surface of a $(d-1)$-dimensional sphere. They are expressed succinctly in radial coordinates as Dirac delta functions. We show results pertaining to distributional solutions that demonstrate a significant but as of yet unexplored domain of study. We begin in section 2 by explaining the pseudo-inverse formulation of the problem, which provides a numerically stable framework for working with spherical shell solutions. In section 3, we formally demonstrate that all distributions containing spherical shells lie in a basin of attraction of solutions to the radially symmetric aggregation equation for $b \in (1-d, a)$. This result is fully rigorous as soon as a gradient flow formulation for the equation in radial coordinates (1.2) allowing general radial measures as initial data exists.

Section 4 presents some exact solutions for spherical shell initial data when $a = 2$ and special cases for $a = 3, 4$. We also show exponential convergence of the interaction energy under suitable assumptions. Section 5 focuses on a new approach for studying problems where the initial data is a convex combination of spherical shells. Specifically, we derive an associated ODE system and prove existence and uniqueness of solutions. In section 6, we explore stability results for the steady state $\delta_{R_{ab}}$ in the context of this ODE system. In particular, we characterize the ODE system as a gradient flow of the energy functional restricted to the appropriate class of solutions. We then show that $\delta_{R_{ab}}$ is a local minimum of this discrete energy under an appropriate assumption on the parameters. Moving to section 7, we fully characterize steady states for parameters $a = 2$ and $b = 2 - d$ and then demonstrate the convergence of these steady states to the continuous case as the number of spherical shells grows arbitrarily large. These sections allow us to conjecture that the rigorous gradient flow formulation of the aggregation equation in radial coordinates (1.2) should extend for exponents $b > 1 - d$, which is left for future exploration.

2. Pseudo-inverse approach. We consider many situations involving initial conditions and/or equilibrium solutions that are spherical shells. The numerics involved can become difficult to handle using standard techniques. One approach to avoid these problems is to recast the PDE in terms of the pseudo-inverse of the corresponding cumulative distribution function (CDF) to the density ρ as proposed in [14, 25, 36, 32]. We outline this process here.

For the particle density $\rho(t, r)$, define its corresponding CDF, $F(t, r)$, as

$$F(t, r) = \int_0^r \rho(t, s) ds.$$

The pseudo-inverse of this function, $\varphi(t, \xi)$ for $\xi \in [0, 1]$, is defined as

$$\varphi(t, \xi) = \inf \left\{ r \in \mathbb{R}_+ \mid F(t, r) \geq \xi \right\}.$$

Since $F(t, r)$ is nondecreasing and càdlàg with respect to r, the function $\varphi(t, \xi)$ is similarly nondecreasing and càdlàg in ξ. If $F(t, r)$ is strictly increasing in r, then $\varphi(t, \xi)$ is precisely its

inverse function. That is, $\varphi(t, F(t, r)) = r$. The corresponding PDE for $\varphi(t, \xi)$ can be derived using this relationship.

We start by noting that

$$0 = \frac{dr}{dt} = \frac{d}{dt}\varphi(t, F(t, r)) = \frac{\partial \varphi}{\partial t}(t, F(t, r)) + \frac{\partial \varphi}{\partial \xi}(t, F(t, r))\frac{\partial F}{\partial t}(t, r).$$

Using the same relationship, we compute the derivative with respect to r:

$$1 = \frac{dr}{dr} = \frac{d}{dr}\varphi(t, F(t, r)) = \frac{\partial \varphi}{\partial \xi}(t, F(t, r))\frac{\partial F}{\partial r}(t, r) = \frac{\partial \varphi}{\partial \xi}(t, F(t, r))\rho(t, r).$$

From the definition of $F(t, r)$ and the PDE for $\rho(t, r)$, we conclude that

$$\frac{d}{dt}F(t, r) = \frac{d}{dt}\int_0^r \rho(t, s)\ ds = \int_0^r \frac{\partial \rho}{\partial t}(t, s)\ ds$$
$$= -\int_0^r \frac{\partial}{\partial s}\left(\rho(t, s)v(t, s)\right)\ ds = -\rho(t, r)v(t, r) + \rho(t, 0)v(t, 0).$$

The quantity $v(t, 0)$ is identically zero. This is best shown geometrically in [10]. They argue that given the radial symmetry of $W(x)$, its gradient $\nabla W(x)$ has vanishing integral along any sphere as the values at antipodal points cancel each other. Since $\rho(t, r)$ is also radially symmetric, this relationship is preserved in the velocity term.

Putting all of this information together, we are left with the equation

$$0 = \frac{\partial \varphi}{\partial t}(t, F(t, r)) - v(t, r) = \frac{\partial \varphi}{\partial t}(t, F(t, r)) - \int_0^\infty \omega(r, s)\rho(t, s)\ ds$$
$$= \frac{\partial \varphi}{\partial t}(t, F(t, r)) - \int_0^\infty \omega(r, s)\frac{\partial F}{\partial s}(t, s)\ ds.$$

Using the substitutions $\varphi(t, F(t, r)) = r$, $\varphi(t, F(t, s)) = s$, $\xi = F(t, r)$, and $\zeta = F(t, s)$, we concisely write the evolution equation for the pseudo-inverse as

$$(2.1) \qquad \frac{\partial \varphi}{\partial t} = \int_0^1 \omega\left(\varphi(t, \xi), \varphi(t, \zeta)\right) d\zeta.$$

To see the numerical stability advantages of this approach, consider how a Dirac delta function appears in pseudo-inverse form. Let $\rho(r) = \delta_R(r)$. The corresponding CDF for this density will be $F(r) = u_R(r)$, the Heaviside function shifted to R. Namely,

$$u_R(r) = \begin{cases} 1, & r > R, \\ 0, & r < R. \end{cases}$$

By definition, the pseudo-inverse is

$$\varphi(\xi) = \begin{cases} R, & \xi \in (0, 1], \\ 0, & \xi = 0. \end{cases}$$

Since we are integrating $\varphi(\xi)$ with respect to the Lebesgue measure, we may ignore sets of measure zero. From a numerical perspective, the pseudo-inverse corresponding to a spherical shell is simply a constant function. The numerical stability advantages of dealing with constant functions on $[0,1]$ over delta functions on $[0,\infty)$ should be obvious.

The pseudo-inverse formulation of the aggregation equation will be crucial to deriving several results in this paper. In addition to the numerical stability properties, the analytic reframing of this method makes it a powerful tool of investigation.

3. Spherical shell dynamics: A variational indication. We will expand upon the current literature by showing the existence of a basin of attraction of solutions in the space of radially symmetric probability distributions. We will demonstrate that distributions formed by spherical shells will evolve by having the radius of the spherical shells simply expand or contract if $b > 3 - d$. This will be fully achieved in sections 5 and 6.

Here we first give an indication based on variational arguments that the result should hold for general radial densities having a spherical shell concentration. The claim is that if a radial initial data has a spherical shell at any location, this spherical shell will evolve by contracting or expanding in time. Our argument centers on examining perturbations of the energy functional. Recall that in [2, 23, 24, 56], the aggregation equation is a gradient flow of the interaction energy in the space of probability distributions with finite second moments equipped with the 2-Wasserstein metric, denoted by $\mathcal{P}_2(\mathbb{R}^d)$.

Technical assumptions on the potential require that it be λ-convex and sufficiently non-singular for a gradient flow theory to be fully rigorous for general measures as initial data. In particular, these assumptions require the repulsive strength $b \geq 2$. No well-posedness result for general measures as initial data is known for the range $-d < b < 2$.

However, restricting oneself to the radial setting clearly improves the regularity of the kernel $\omega(r,s)$ involved in the velocity field (1.2). In fact, using [5] and the computations in Appendix A, the function $\omega(r,s)$ is continuously differentiable in both variables for $r, s > 0$ for $b > 3 - d$ due to additional factor r^{d-1} coming from the radial change of variables. This fact indicates that developing a gradient flow theory leading to well-posedness for general radial measures should be possible for $b > 3 - d$. This is an interesting line of research not pursued in this work. Numerical investigation in sections 5 and 6 suggests that the result extends to the range $b > 1 - d$.

Our claim here is that given a radial density ρ, the velocity field generated by the density via (1.2) is realized taking the directional derivative of the interaction energy in the direction determined by δ_R', formally speaking. Since the velocity field corresponds to the direction of steepest descent of the energy, this indicates that the mass already concentrated at location R should not be able to escape from R without increasing the interaction energy. This computation is purely formal due to the form of the perturbation, but we will substantiate the result in sections 5 and 6 in the case of finite number of spherical shells.

We begin with a perturbation $\mu(r)$ of the energy functional at a fixed time t satisfying $\int_{\mathbb{R}_+} \mu(r)dr = 0$ and having compact support:

$$E[\rho + \varepsilon\mu] = E[\rho] + 2\varepsilon E[\mu, \rho] + \varepsilon^2 E[\mu].$$

We use this perturbation expression to define a new functional $L[\mu]$ that gives the rate of

change for the interaction energy for a density ρ in the direction μ:

$$L[\mu] = \lim_{\varepsilon \to 0} \frac{E[\rho + \varepsilon\mu] - E[\rho]}{\varepsilon} = \lim_{\varepsilon \to 0} \left(2E[\mu, \rho] + \varepsilon E[\mu] \right).$$

To take the limit as $\varepsilon \to 0$ requires that the quantities $E[\mu, \rho]$ and $E[\mu]$ be well-defined and finite. We remark that the functional $L[\cdot]$ corresponds to the Gateaux derivative of the interaction energy. Nearly identical expressions can be found in [4, 16].

The directional ansatz we wish to plug into this expression is $\mu(r) = \delta'_R(r)$. Direct substitution yields

$$\begin{aligned}
E[\delta'_R] &= \frac{1}{2\omega_d} \iint_{\mathbb{R}_+^2} \int_{\partial B(0,1)} W(re_1 - s\eta) d\sigma(\eta) \delta'_R(r) \delta'_R(s) dr ds \\
&= -\frac{1}{2\omega_d} \int_{\mathbb{R}_+} \int_{\partial B(0,1)} e_1 \cdot \nabla W(Re_1 - s\eta) d\sigma(\eta) \delta'_R(s) ds = -\frac{1}{2} \partial_2 \omega(R, R)
\end{aligned}$$

and

$$\begin{aligned}
2E[\delta'_R, \rho] &= \frac{1}{\omega_d} \iint_{\mathbb{R}_+^2} \int_{\partial B(0,1)} W(re_1 - s\eta) d\sigma(\eta) \delta'_R(r) \rho(s) \, dr ds \\
&= -\frac{1}{\omega_d} \int_{\mathbb{R}_+} \int_{\partial B(0,1)} e_1 \cdot \nabla W(Re_1 - s\eta) d\sigma(\eta) \rho(s) \, ds \\
&= \int_{\mathbb{R}_+} \omega(R, s) \rho(s) \, ds = v(R).
\end{aligned}$$

The quantity $E[\delta'_R]$ is finite for $b > 3 - d$ and infinite for $b \le 3 - d$. The quantity $E[\delta'_R, \rho]$ will be infinite when $b \le 1 - d$ and there is a spherical shell with radius R.

Assuming first that $b > 3 - d$, the velocity at each radius R is generated by evolving in the direction δ'_R. For distributions containing a spherical shell with radius R_0, this direction corresponds to an instantaneous contraction/expansion of the shell. Thus, at any given time a spherical shell is expected to shrink/grow to a spherical shell of smaller/larger radius.

The result extends to $b \in (1 - d, 3 - d]$, but the argument requires more subtlety. The limit in the expression for $L[\mu]$ has an indeterminant form. Consider approximating the ansatz

$$\mu_\lambda(r) = \begin{cases} \frac{1}{\lambda^2}, & R - \lambda < r < R, \\ -\frac{1}{\lambda^2}, & R < r < R + \lambda, \\ 0 & \text{otherwise} \end{cases}$$

for $0 < \lambda < R$. Plugging in the approximations and using the nonradial formulation (see (1.1) from section 1),

$$E[\mu_\lambda] = \frac{1}{2} \iint_{\mathbb{R}^d \times \mathbb{R}^d} \left[\frac{|x - y|^a}{a} - \frac{|x - y|^b}{b} \right] \left[\frac{\mu_\lambda(|x|)}{\omega_d |x|^{d-1}} \right] \left[\frac{\mu_\lambda(|y|)}{\omega_d |y|^{d-1}} \right] dx dy.$$

From this comes the inequality

$$|E[\mu_\lambda]| \le \frac{1}{2\omega_d^2 \lambda^4} \left[\iint_D \frac{|x - y|^a}{|a||x|^{d-1}|y|^{d-1}} dx dy + \iint_D \frac{|x - y|^b}{|b||x|^{d-1}|y|^{d-1}} dx dy \right],$$

where $D = \{x, y \in \mathbb{R}^d \mid R - \lambda < |x|, |y| < R + \lambda\}$. If a and b are positive, then the integrals are clearly bounded. As such, suppose $b < 0$; then

$$\iint_D \frac{|x - y|^b}{|b||x|^{d-1}|y|^{d-1}} dx dy \leq \iint_D C|x - y|^b dx dy, \qquad C = \frac{1}{|b||R - \lambda|^{2(d-1)}}.$$

This integral is finite for $b > -d$. Since $a > b$, the associated integral to a will also be finite regardless of sign.

For each $\lambda \in (0, R)$, $L[\mu_\lambda] = 2E[\mu_\lambda, \rho]$ is well-defined and finite. $E[\delta'_R, \rho]$ is also well-defined and finite for $b > 1 - d$. To compute the limit, first define the antiderivative

$$\Omega(r, s) = \int \frac{1}{\omega_d} \int_0^\infty \int_{\partial B(0,1)} W(re_1 - s\eta) d\sigma(\eta) \rho(s) ds dr.$$

Then, letting $\lambda \to 0$,

$$\begin{aligned}
\lim_{\lambda \to 0} L[\mu_\lambda] &= \lim_{\lambda \to 0} 2E[\mu_\lambda, \rho] \\
&= \lim_{\lambda \to 0} \frac{1}{\omega_d} \iint_{\mathbb{R}^2_+} \int_{\partial B(0,1)} W(re_1 - s\eta) d\sigma(\eta) \mu_\lambda(r) \rho(s) dr ds \\
&= \lim_{\lambda \to 0} \frac{1}{\lambda^2} \left[\int_{R-\lambda}^R \frac{1}{\omega_d} \int_0^\infty \int_{\partial B(0,1)} W(re_1 - s\eta) d\sigma(\eta) \rho(s) ds dr \right. \\
&\qquad \left. - \int_R^{R+\lambda} \frac{1}{\omega_d} \int_0^\infty \int_{\partial B(0,1)} W(re_1 - s\eta) d\sigma(\eta) \rho(s) ds dr \right] \\
&= \lim_{\lambda \to 0} \frac{[\Omega(R, s) - \Omega(R - \lambda, s)] - [\Omega(R + \lambda, s) - \Omega(R, s)]}{\lambda^2} \\
&= \lim_{\lambda \to 0} \frac{-\Omega(R + \lambda, s) + 2\Omega(R, s) - \Omega(R - \lambda, s)}{\lambda^2} \\
&= -\left. \frac{\partial^2}{\partial r^2} \right|_{r=R} \Omega(r, s) = \int_0^\infty \omega(R, s) \rho(s) ds = 2E[\delta'_R, \rho].
\end{aligned}$$

Thus, the result is extended to $b > 1 - d$.

This variational argument cannot hold for $b \in (-d, 1-d]$. In this range, the function $\omega(r, s)$ is properly singular along the diagonal. As such, no density of particles may concentrate on a spherical shell. Doing so would produce an infinite instantaneous velocity term.

Notably, the previous proof is kernel independent in the following sense: as long as the corresponding $\omega(r, s)$ function for a kernel is well-defined on the diagonal, this argument holds. This is especially noteworthy for regularized kernels $W_\varepsilon(x) = \psi_\varepsilon * W * \psi_\varepsilon(x)$, where $\psi_\varepsilon(x) = \varepsilon^{-d} \psi\left(\frac{x}{\varepsilon}\right)$ is an appropriate mollifier for the kernel; i.e., ψ is a positive, radially symmetric, smooth function with unit integral. Regularized kernels appear, for example, in [27, 26] in a blob method for the particle model. Such kernels may be used to approximate singular kernels and extend the range of the parameter b in which numerical methods are viable.

The spherical shell dynamics lie at the heart of the rest of the results. We will show that convex combinations of spherical shells will have steady states that are also convex

combinations, with possibly less different radii, of spherical shells in sections 5 and 6 for $b > 3 - d$. We remind the reader that $\delta_{R_{ab}}$ is the only steady state solution for single spherical shell initial data when $b \in (1 - d, a)$ as shown in [5]. It remains an open problem whether other types of distributional solutions may also constitute part of the basin of attraction.

4. Exact solutions and exponential convergence of the entropy/interaction energy. As mentioned, some immediate consequences follow the existence of this basin of attraction. For certain parameter values, we can find exact solutions to the aggregation equation when the initial data is a spherical shell. We articulate this precisely in the following corollary. From section 3, $\varphi(t, \xi) = R(t)$ for a single spherical shell. The pseudo-inverse equation (2.1) then reduces to the ODE

$$(4.1) \qquad \frac{dR}{dt} = \omega(R, R) = c(a, d)R^{a-1} - c(b, d)R^{b-1},$$

with $c(x, d)$ defined by (A.1). Note that for $x > 1 - d$ and $d \geq 2$, $c(x, d) < 0$. We remark that R_{ab}, defined in (1.5), is the root of the right-hand side and refer the reader to Appendix A for calculations involving ω.

Theorem 4.1. *Let $R(0) = R_0$, and let R_{ab} be given by* (1.5):
1. *If $a = 2$ and $b \in (1 - d, a)$, then*

$$R(t) = \left[R_{ab}^{2-b} \left(1 - e^{(2-b)c(2,d)t} \right) + R_0^{2-b} e^{(2-b)c(2,d)t} \right]^{\frac{1}{2-b}}.$$

2. *If $a = 3$ and $b = 2$, then*

$$R(t) = \frac{R_{ab}}{1 + \left(\frac{R_{ab}}{R_0} - 1 \right) e^{c(3,d)R_{ab}t}}.$$

3. *If $a = 3$ and $b = 1$, then*

$$R(t) = \left(\frac{1 + ke^{2c(3,d)R_{ab}t}}{1 - ke^{2c(3,d)R_{ab}t}} \right) R_{ab}, \quad k = \frac{R_0 - R_{ab}}{R_0 + R_{ab}}.$$

4. *If $a = 4$ and $b = 2$, then*

$$R(t) = R_{ab}R_0 \left[R_0^2 \left(1 - e^{2c(4,d)R_{ab}^2 t} \right) + R_{ab}^2 e^{2c(4,d)R_{ab}^2 t} \right]^{-1/2}.$$

Proof. (1) Let $a = 2$, and let $R(0) = R_0$. Equation (4.1) reduces to the ODE

$$\frac{dR}{dt} = c(2, d)R - c(b, d)R^{b-1} = c(2, d)R^{b-1} \left(R^{2-b} - R_{ab}^{2-b} \right).$$

Then

$$\int \frac{R^{1-b}}{R^{2-b} - R_{ab}^{2-b}} dR = \int c(2, d)dt.$$

Using the substitution $u = R^{2-b} - R_{ab}^{2-b}$, we have $du = (2-b)R^{1-b}dR$. Therefore, we deduce that $R^{2-b} - R_{ab}^{2-b} = (R_0^{2-b} - R_{ab}^{2-b})e^{(2-b)c(2,d)t}$ after basic calculus, finally yielding

$$R(t) = \left[R_{ab}^{2-b} \left(1 - e^{(2-b)c(2,d)t} \right) + R_0^{2-b}e^{(2-b)c(2,d)t} \right]^{\frac{1}{2-b}}.$$

(2) For $a = 3$ and $b = 2$,
$$\frac{dR}{dt} = c(3,d)R(R - R_{ab}).$$

From this,

$$\frac{dR}{R(R - R_{ab})} = c(3,d)dt \quad \Rightarrow \quad R(t) = \frac{R_{ab}}{\left(\frac{R_{ab}}{R_0} - 1 \right)e^{c(3,d)R_{ab}t} + 1}.$$

(3) When $a = 3$ and $b = 1$,

$$\frac{dR}{dt} = c(3,d)(R^2 - R_{ab}^2) \quad \Rightarrow \quad \frac{dR}{(R - R_{ab})(R + R_{ab})} = c(3,d)dt.$$

We then deduce that

$$\int \frac{1}{R - R_{ab}} - \frac{1}{R + R_{ab}} \, dR = \int 2c(3,d)R_{ab}dt \quad \Rightarrow \quad R(t) = \left(\frac{1 + ke^{2c(3,d)R_{ab}t}}{1 - ke^{2c(3,d)R_{ab}t}} \right) R_{ab}.$$

(4) We turn now to $a = 4$ and $b = 2$:

$$\frac{dR}{dt} = c(4,d)R(R^2 - R_{ab}^2) \quad \Rightarrow \quad \int \frac{dR}{R(R - R_{ab})(R + R_{ab})} = \int c(4,d)dt.$$

Using partial fraction decomposition as above, integrating and using basic algebra leads to the stated formula. ∎

When applying the previous procedure to cases where $a > 2$ and b is outside the parameters given, explicit expressions are not possible. Problems involving convex combinations of spherical shells as initial data must generally be dealt with using other techniques since the interactions between spherical shells sufficiently complicate the differential equations.

While for many parameter choices explicit solutions cannot be given, some qualitative behavior can be deduced. We demonstrate in this section that for certain parameter choices with spherical shell initial data, solutions converge exponentially fast to the steady state. Consequently, the corresponding energy also converges exponentially fast.

We again use the pseudo-inverse equation to prove these convergence results. We remark that in the one-dimensional and radial cases, convergence of measures in the p-Wasserstein distance corresponds to convergence of their respective pseudo-inverses in L^p-distances. Since the pseudo-inverse is merely a scalar here, all L^p-norms reduce to absolute value.

Theorem 4.2. *For $a > 1 - d$, $b \in (1 - d, a)$, $d \geq 2$, and $\varphi(0, \xi) = R_0$, the pseudo-inverse solution converges exponentially fast to the steady state.*

Proof. Recall that for spherical shell initial data, the equation takes the form of (4.1):

$$\frac{dR}{dt} = f(R), \qquad f(R) = c(a, d)R^{a-1} - c(b, d)R^{b-1}.$$

For $R > 0$, this has the unique steady state $R = R_{ab}$. Consider the derivative of f evaluated at the fixed point

$$f'(R_{ab}) = c(a, d)R_{ab}^{a-b}(a - b).$$

This term must be negative when $a > 1 - d$ based on (A.1). By the standard linearization theorem for dynamical systems (see [58], for example), there exists a neighborhood of the unique steady state within which solutions will converge exponentially fast. Taking into account that the right-hand side of (4.1) changes sign only once at R_{ab}, and then solutions are increasing (resp., decreasing) for $0 < R_0 < R_{ab}$ (resp., for $R_0 > R_{ab}$). Thus, all solutions converge exponentially fast to R_{ab}. ∎

Corollary 4.3. *The entropy/interaction energy also converges exponentially fast.*

Proof. Consider the dissipation in the pseudo-inverse form

$$\frac{d}{dt}E[\varphi](t) = -\int_0^1 \left(\frac{\partial \varphi}{\partial t}(t, \xi)\right)^2 d\xi.$$

We deduce from $\varphi(t, \xi) = R(t)$ that

$$\frac{d}{dt}E[\varphi](t) = -\omega(R(t), R(t))^2 = -\omega(R(t), R(t))R'(t).$$

Integrating both sides gives

$$-\int_t^\infty \frac{d}{ds}E[R](s)ds = c(a, d)\int_t^\infty R^{a-1}(s)R'(s)ds - c(b, d)\int_t^\infty R^{b-1}(s)R'(s)ds$$
$$\Rightarrow \ E[R](t) - E[R_{ab}] = c(a, d)[R^a(t) - R_{ab}^a] - c(b, d)[R^b(t) - R_{ab}^b].$$

The right-hand side may be rewritten as

$$\text{sgn}(R(t) - R_{ab})\left[-c(a, d)\left(\frac{R^a(t) - R_{ab}^a}{R(t) - R_{ab}}\right) + c(b, d)\left(\frac{R^b(t) - R_{ab}^b}{R(t) - R_{ab}}\right)\right]|R(t) - R_{ab}|.$$

Invoking the inequality $|R(t) - R_{ab}| \leq ke^{-C_1 t}$,

$$E[R](t) \leq E[R_{ab}] + C_2|R(t) - R_{ab}| \leq E[R_{ab}] + C_2 ke^{-C_1 t},$$

where $C_2 > 0$ depends on a, b, d, $R(0)$, and T. Thus, the entropy/interaction energy converges exponentially fast to that of the steady state. ∎

5. ODE system for convex combinations of spherical shells.

We turn our attention to problems where the initial distribution of particles is a convex combination of spherical shells. We write initial data for convex combinations of spherical shells as

$$\rho(0, r) = \sum_{i=1}^{N} \alpha_i \delta_{R_i}(r), \quad \sum_{i=1}^{N} \alpha_i = 1, \quad \alpha_i \in (0, 1), \quad R_i < R_{i+1}.$$

The last assumption can be made without loss of generality for convenience by simply relabeling the shells. By the variational indication in section 3, we expect each spherical shell to retain its respective weight α_i. In fact, each spherical shell should evolve simply by expanding or contracting. In other words, the spherical shells should not split at least when $b > 3 - d$, where we recall the critical value b^* is given by (1.5). We will also give numerical evidence that supports this to happen for $b > 1 - d$. Therefore, the number of spherical shells cannot increase. We look for solutions that may be written as

$$\rho(t, r) = \sum_{i=1}^{N} \alpha_i \delta_{R_i(t)}(r), \quad \sum_{i=1}^{N} \alpha_i = 1, \quad \alpha_i \in (0, 1).$$

From this result it follows that the equilibrium solutions for $b \in (1 - d, b^*)$ depend on both n and the specific set of α_i's. Thus, for each n there is an uncountable family of equilibrium solutions. To explore these solutions, we turn to another perspective particular to this specific case. Namely, the aggregation equation with an initial condition given as a convex combination of spherical shells reduces to a system of ODEs, each one governing one of the spherical shells. We derive this system now using the pseudo-inverse formulation.

Consider an initial particle density of the previous form. The corresponding pseudo-inverse solution will have the form

$$\varphi(t, \xi) = \sum_{i=1}^{N} \chi_i(\xi) R_i(t), \quad \chi_i(\xi) = \chi_{(\beta_{i-1}, \beta_i)}(\xi), \quad \beta_i = \sum_{j=1}^{i} \alpha_j.$$

Each χ_i represents a characteristic function on the ξ axis. Note that they are all defined on disjoint sets. We take $\beta_0 = 0$. Clearly, the following relationships hold:

$$\frac{\partial \varphi}{\partial t}(t, \xi) = \sum_{i=1}^{N} \chi_i(\xi) R_i'(t)$$

and

$$\chi_j(\xi) \frac{\partial \varphi}{\partial t}(t, \xi) = \chi_j(\xi) \sum_{i=1}^{N} \chi_i(\xi) R_i'(t) = \chi_j(\xi) R_j'(t).$$

We now use these relationships and the evolution of the pseudo-inverse to solve for each $R_i'(t)$:

$$\frac{\partial \varphi}{\partial t}(t, \xi) = \int_0^1 \omega\left(\varphi(t, \xi), \varphi(t, \zeta)\right) d\zeta = \sum_{i=1}^{N} \int_{\beta_{i-1}}^{\beta_i} \omega\left(\varphi(t, \xi), R_i(t)\right) d\zeta$$

$$= \sum_{i=1}^{N} \alpha_i \omega\left(\varphi(t, \xi), R_i(t)\right)$$

and

$$\chi_j(\xi)\frac{\partial\varphi}{\partial t}(t,\xi) = \sum_{i=1}^{n}\alpha_i\chi_j(\xi)\omega\left(R_j(t),R_i(t)\right).$$

We reformulate the evolution equation for $\varphi(t,\xi)$ as the system of ODEs

$$R_j'(t) = \sum_{i=1}^{N}\alpha_i\omega\left(R_j(t),R_i(t)\right), \qquad j=1,\ 2,\ldots,N.$$

Such a system resembles an empirical distribution as seen at the kinetic level. In this case, the delta functions are in radial coordinates. We take a moment to compare and contrast convex combinations of spherical shells with empirical distributions.

The formal similarity of the two distributions produces some common properties. For example, each distribution corresponds to a simplified and discretized picture that approaches, in the distributional sense, continuous results when the number of "particles" is allowed to grow arbitrarily large. However, each spherical shell "particle" is technically a uniform distribution of particles on a sphere. As such, these distributions are truly continuous despite their discrete appearance. One consequence of this fact is that spherical shells interact with themselves in their evolution while individual particles do not. Furthermore, the evolution equations and energies have different forms.

Some similarity can be seen with the work of Fellner and Raoul on convex combinations of delta functions in the nonradial, one-dimensional case [32]. In their case, particles that are concentrated at points move along a line, as opposed to the present work where particles concentrated on spheres expand or contract in dimension 2 or 3.

We now examine the problem from an ODE perspective. Considering the right-hand side of the expression, we investigate the properties of $\omega(r,s)$ to demonstrate that the problem is well-posed.

Theorem 5.1. *The initial value problem associated to the system of differential equations*

$$(5.1) \qquad R_j'(t) = \sum_{i=1}^{N}\alpha_i\omega(R_j(t),R_i(t)), \qquad j=1,2,\ldots,N,$$

is well-posed for $b \in (3-d,a)$ for initial data satisfying $R_i(0) \neq R_j(0)$ for $i \neq j$. Thus, a solution exists and up to its maximal time of existence is unique. Furthermore, if $b \geq 2$, then the minimal radius remains strictly positive for all times.

Proof. From [5] and the computations in Appendix A, the function $\omega(r,s)$ is continuously differentiable in both variables $r,s > 0$ for $b > 3-d$. The result follows immediately from Picard's theorem for ODE systems (see [58] for reference). If $b \geq 2$, ω is continuously differentiable up to $r = s = 0$ and $\omega(0,0) = 0$ being an equilibrium point of the system. The uniqueness part of Picard's theorem implies the last statement. ∎

In section 6, we will see that solutions additionally remain bounded in $\mathbb{R}_+$ for all time. As a consequence, existence and uniqueness of solutions applies for all time and no merging

of spherical shells can occur for a positive radius. If two shells were to merge, that would invalidate uniqueness of the solution, as those two shells could be recharacterized as a single shell and the reverse time evolution could not be recovered.

We also remark that the exponent $3-d$ is quite natural in a sense because when switching to radial coordinates, as in section 1, one multiplies by a factor of $\omega_d r^{d-1}$. As such, $|x|^{d-1}|x|^{3-d} = |x|^2$, where $|x|^2$ is the minimal power satisfying the previously mentioned local Lipschitz condition in the nonradial formulation.

The result of Theorem 5.1 extends somewhat to the range of values $b \in (1-d, 3-d]$. To see this, denote $X = (0, \infty) \times (0, \infty)$ and $D = \{(x, y) \in X \mid x = y\}$. The partial derivatives of $\omega(r, s)$ are well-defined and continuous on $(r, s) \in X \setminus D$. Thus, $\omega(r, s)$ is Lipschitz continuous on $X \setminus D$. For $(r, s) \in D$, we may rewrite the expression as

$$\omega(r, r) = f(r) = c(a, d)r^{a-1} - c(b, d)r^{b-1}.$$

The function f is continuously differentiable on $(0, \infty)$ and thus Lipschitz continuous. The function f accounts for the self-interactions of the spherical shells. Since the sum of Lipschitz continuous functions is also Lipschitz continuous, the right-hand side of the ODE system is Lipschitz continuous as long as $R_i \neq R_j$ for $i \neq j$. A consequence of the Cauchy–Lipschitz theory is the well-posedness of a solution to the spherical shells equations (5.1) up to a maximal time of existence.

Remark 5.2. Notice that the maximal time of existence is fully characterized by either the time two different spherical shells collide or the radius of the largest spherical shell escapes to infinity or the radius of the smallest spherical shell converges to zero. The collision corresponds to the possibility of the system entering a state where the ODE is ill-defined since ω fails to be Lipschitz continuous (indeed, continuous at all for $b \leq 2 - d$). We have not observed any of the three in the numerical simulations.

We confirm these results numerically using the pseudo-inverse formulation; see Figure 2. When initial data corresponding to convex combinations of spherical shells is implemented, the numerical evolution corresponds to the expansion/contraction dynamics. The shells tend to converge to $\delta_{R_{ab}}$ when $b \in (b^*, a)$, but numerical results suggest the possibility of other steady states for at least some parameter settings. When $b \in (1 - d, b^*)$, the shells converge to steady states with the number of shells and mass distribution conserved. None of these steady states has previously been explored to our knowledge.

Given the well-posedness of the system of spherical shells, several questions arise about the evolution of the system and the relationship to the continuous case. To what extent does the evolution of the system approximate the evolution of continuous densities in the distributional sense? What precisely are the steady states of the system? Do they converge in an appropriate topology to the (global) minimizers of the energy functional? Answering these questions may ultimately shed light on continuous solutions in parameter regimes that have eluded analytic investigation. They are also interesting in their own right.

6. Gradient flow structure and asymptotics of spherical shells. We begin investigating the steady states for the ODE system by first considering the single spherical shell steady state $\delta_{R_{ab}}$. We begin by first plugging in a spherical shell density into the radial form of the
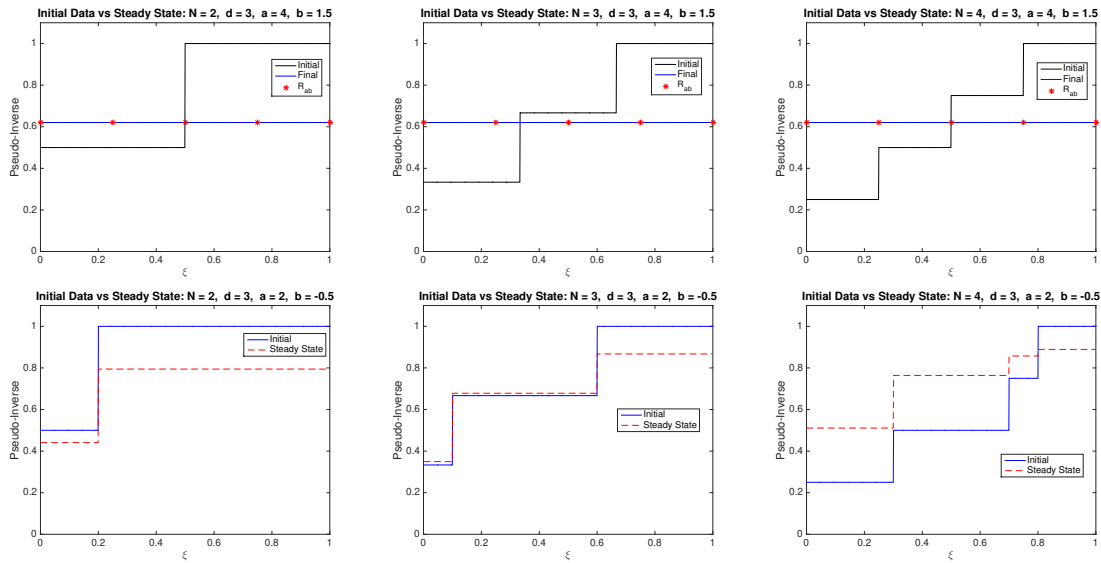
Figure 2. *Pseudo-inverse initial data versus steady states for $d = 3$, $a = 4$, $b = 1.5$ and $d = 3$, $a = 2$, $b = -0.5$ with varying numbers of spherical shells. Note that the top range converges to $\delta_{R_{ab}}$ while the bottom range converges to other spherical shell steady states.*

energy functional given by (1.4). Explicitly, given

$$\rho(t,r) = \sum_{i=1}^{N} \delta_{R_i(t)}(r), \quad \alpha_i \in (0,1), \quad \sum_{i=1}^{N} \alpha_i = 1,$$

the energy functional takes the form

$$
\begin{aligned}
E[\rho](t) &= \frac{1}{2\omega_d} \iint_{\mathbb{R}_+^2} \int_{\partial B(0,1)} W(re_1 - s\eta)d\sigma(\eta)\rho(t,r)\rho(t,s)drds \\
&= \frac{1}{2\omega_d} \iint_{\mathbb{R}_+^2} \int_{\partial B(0,1)} W(re_1 - s\eta)d\sigma(\eta)\left(\sum_{i=1}^{N} \alpha_i \delta_{R_i(t)}(r)\right)\left(\sum_{j=1}^{N} \alpha_j \delta_{R_j(t)}(s)\right)drds \\
&= \frac{1}{2\omega_d} \sum_{i,j=1}^{N} \alpha_i \alpha_j \int_{\partial B(0,1)} W(R_i(t)e_1 - R_j(t)\eta)d\sigma(\eta).
\end{aligned}
$$

For this special case, we will denote the energy function by $E[R](t)$, where R is the column vector containing the radii. Taking the derivative of the energy function with respect to a

given radius yields

$$
(6.1) \qquad \frac{\partial E}{\partial R_k}[R] = \frac{1}{2\omega_d} \left(-\sum_{i=1}^{N} \alpha_i \alpha_k \int_{\partial B(0,1)} \eta \cdot \nabla W(R_i e_1 - R_k \eta) d\sigma(\eta) \right.
$$

$$
\left. + \sum_{j=1}^{n} \alpha_k \alpha_j \int_{\partial B(0,1)} e_1 \cdot \nabla W(R_k e_1 - R_j \eta) d\sigma(\eta) \right)
$$

$$
= -\alpha_k \sum_{j=1}^{N} \alpha_j \omega(R_k, R_j).
$$

The second equality comes from using the antisymmetry of ∇W, a change of variables in the spherical coordinate, and relabeling the index i to j in the first sum.

For clarity, we denote by α the column vector containing the probability weights of the spherical shells and by A the diagonal matrix whose nonzero entries are the same respective weights, i.e., $(A)_{ii} = \alpha_i$. Thus, the structure for the system of ODEs is given by

$$
\frac{dR}{dt} = -A^{-1} \nabla_R E[R].
$$

The dynamical system for the shells is a rescaled gradient flow of the energy $E[R]$. The fixed points of the system are then the critical points of the energy function.

Importantly, the energy function $E[R]$ is bounded below. Indeed, the energy functional defined in (1.1) is bounded below since it is easy to check that the radial potential $W(x)$ achieves its minimum for $a > b$ at $|x| = 1$. Thus, $W(x) \geq W_*$ for all x and the energy functional is bounded below on probability measure including a restriction to the subset of radial distributions.

Theorem 6.1. *For $b \in (3 - d, a)$, the ODE system will converge to the set of steady states of the associated energy function.*

Proof. Given the gradient structure of the ODE system, we wish to invoke the LaSalle invariance principle; see [58]. To do so, we must show that no solutions contain components escaping to infinity. It suffices then to show that the largest radius remains bounded for all time.

To see the confinement of the radii, note from Appendix A that the function ω may be written as

$$
\omega(r, s) = r^{b-1} \psi_b \left(\frac{s}{r} \right) - r^{a-1} \psi_a \left(\frac{s}{r} \right),
$$

$$
\psi_x(\tau) = \frac{\omega_{d-1}}{\omega_d} \int_0^{\pi} (1 - \tau \cos\theta)(1 + \tau^2 - 2\tau \cos\theta)^{x/2-1} \sin^{d-2}\theta \, d\theta.
$$

Using the assumption that $R_i(0) < R_{i+1}(0)$ and that merging does not occur for $b \in (3-d, a)$,

we consider

$$\frac{dR_N}{dt}(t) = \sum_{j=1}^{N} \alpha_j \omega(R_N(t), R_j(t))$$

$$= \sum_{j=1}^{N} \alpha_j \left[R_N^{b-1}(t)\psi_b\left(\frac{R_j(t)}{R_N(t)}\right) - R_N^{a-1}(t)\psi_a\left(\frac{R_j(t)}{R_N(t)}\right) \right].$$

Since $0 \le R_j(t) \le R_N(t)$, we must consider the function $\psi_x(\tau)$ on $[0,1]$. From Lemma A.1, we have that ψ_x is continuous in τ with $\psi_x(0) = 1$. Furthermore, ψ_x is nondecreasing on $[0,1]$ for $x > 2$, constant on $[0,1]$ for $x = 2$, and nonincreasing on $[0,1]$ for $3 - d < x < 2$.

Using the constants

$$k_a = \begin{cases} 1, & 2 \le b < a, \\ 1, & 3 - d < b < 2 \le a, \\ \psi_a(1), & 3 - d < b < a < 2, \end{cases} \qquad k_b = \begin{cases} \psi_b(1), & 2 \le b < a, \\ 1, & 3 - d < b < 2 \le a, \\ 1, & 3 - d < b < a < 2, \end{cases}$$

we obtain the inequality

$$\frac{dR_N}{dt} \le \sum_{j=1}^{N} \alpha_j \left[R_N^{b-1} k_b - R_N^{a-1} k_a \right] = R_N^{b-1}\left(k_b - R_N^{a-b} k_a \right).$$

The critical points of the right-hand side are $R_N = 0$ and $R_N = (k_b/k_a)^{\frac{1}{a-b}}$ (which we will denote by $R^\dagger$). For $R_N(0) \in (0, R^\dagger)$, the radius is bounded by the fact that the right-hand side will vanish as $R_N(t)$ approaches $R^\dagger$. If $R_N(0) > R^\dagger$, then the derivative is strictly negative and $R_N(t)$ will decrease. As such, $R_N(t)$ is bounded by $\max\left\{ R_N(0), R^\dagger \right\}$. Thus, the result is shown. Notice that $R_1(t) > 0$ for all times if $b \ge 2$; however, we cannot prevent $R_1(t)$ from converging to 0 asymptotically as $t \to \infty$. Even more for $3 - d < b < 2$, the function ω is not differentiable at 0, so we cannot prevent $R_1(t)$ from touching 0 in finite time. Observe that $R_1 = \cdots = R_N = 0$ is a stationary state of the problem in this range, and therefore the asymptotic statement also holds in this hypothetical case; see the next remark. ∎

Remark 6.2. In Theorem 5.1, we proved that the smallest radius remains strictly positive for all times for $b > 2$. For $3 - d < b < a < 2$, we can prove the same result in a very specific configuration of the radii. Consider the equation for the derivative of $R_1(t)$. That is,

$$R_1'(t) = \sum_{j=1}^{N} \alpha_j \left[R_1^{b-1}(t)\psi_b\left(\frac{R_j(t)}{R_1(t)}\right) - R_1^{a-1}(t)\psi_a\left(\frac{R_j(t)}{R_1(t)}\right) \right].$$

Then

$$R_1'(t) = R_1(t) \sum_{j=1}^{N} \alpha_j \left[R_1^{b-2}(t)\psi_b\left(\frac{R_j(t)}{R_1(t)}\right) - R_1^{a-2}(t)\psi_a\left(\frac{R_j(t)}{R_1(t)}\right) \right]$$

$$= R_1(t) \sum_{j=1}^{N} \alpha_j \left[R_j^{b-2}(t)\left(\frac{R_1(t)}{R_j(t)}\right)^{b-2}\psi_b\left(\frac{R_j(t)}{R_1(t)}\right) - R_j^{a-2}(t)\left(\frac{R_1(t)}{R_j(t)}\right)^{a-2}\psi_a\left(\frac{R_j(t)}{R_1(t)}\right) \right]$$

$$= R_1(t) \sum_{j=1}^{N} \alpha_j \left[R_j^{b-2}(t)\left(\frac{R_j(t)}{R_1(t)}\right)^{2-b}\psi_b\left(\frac{R_j(t)}{R_1(t)}\right) - R_j^{a-2}(t)\left(\frac{R_j(t)}{R_1(t)}\right)^{2-a}\psi_a\left(\frac{R_j(t)}{R_1(t)}\right) \right].$$

Using that $\lim_{\tau\to\infty} \psi_x(\tau)\tau^{2-x} = \frac{d+x-2}{d}$ from Lemma A.1, we can see that

$$(6.2) \quad \lim_{R_1\to 0} R_j^{b-2}\left(\frac{R_j}{R_1}\right)^{2-b}\psi_b\left(\frac{R_j}{R_1}\right)$$
$$- R_j^{a-2}\left(\frac{R_j}{R_1}\right)^{2-a}\psi_a\left(\frac{R_j}{R_1}\right) = R_j^{b-2}\frac{d+b-2}{d} - R_j^{a-2}\frac{d+a-2}{d}.$$

One way to obtain that $R_1(t) > 0$ is to show that the right-hand side of (6.2) is positive for all $j = 1, \ldots, N$. That is,

$$R_j^{b-2}\frac{d+b-2}{d} - R_j^{a-2}\frac{d+a-2}{d} > 0.$$

Since $R_j(t) < R_{j+1}(t)$, it is sufficient that the inequality is true for the largest radius. Equivalently,

$$R_N(t) < \left(\frac{d+b-2}{d+a-2}\right)^{\frac{1}{a-b}}.$$

Concluding this remark, for $3 - d < b < a < 2$, the smallest radius remains strictly positive if $R_N(t) < \left(\frac{d+b-2}{d+a-2}\right)^{\frac{1}{a-b}}$.

We note that the state where all radii are R_{ab} is always a fixed point. For $b < b^*$, the numerical evidence (see Figure 2 for examples) suggests that solutions converge to a steady state of N spherical shells. Based on Theorem 6.1, we know that steady states of the system exist with support in $[0, R^\dagger]$ and that solutions will converge toward them. However, precisely characterizing these steady states is a nontrivial task we dedicate to future research.

To investigate the stability of $\delta_{R_{ab}}$, we consider the Hessian of $E[R]$, denoted simply by $H[R]$. Its entries are

$$(H[R])_{ii} = -\alpha_i \sum_{k=1}^{N} \alpha_k \partial_1 \omega(R_i, R_k) - \alpha_i^2 \partial_2 \omega(R_i, R_i), \qquad (H[R])_{ij} = -\alpha_i\alpha_j\partial_2\omega(R_i, R_j).$$

Evaluating when all radii are set to R_{ab} yields the symmetric matrix

$$(H[R_{ab}])_{ii} = -\alpha_i\partial_1\omega(R_{ab}, R_{ab}) - \alpha_i^2\partial_2\omega(R_{ab}, R_{ab}), \qquad (H[R_{ab}])_{ij} = -\alpha_i\alpha_j\partial_2\omega(R_{ab}, R_{ab}).$$

Using some simple algebra, we determine that $H[R_{ab}]$ has the form

$$H[R_{ab}] = -\partial_1\omega(R_{ab}, R_{ab})A - \partial_2\omega(R_{ab}, R_{ab})\alpha\alpha^T,$$

where the superscript T denotes the transpose. We now show that this Hessian evaluated at the fixed point is positive definite for a certain range of the parameters. To that end, consider the quadratic form

$$x^T H[R_{ab}]x = -\partial_1\omega(R_{ab}, R_{ab})x^T A x - \partial_2\omega(R_{ab}, R_{ab})x^T \alpha\alpha^T x$$

$$= -\partial_1\omega(R_{ab}, R_{ab})\sum_{i=1}^{N}\alpha_i x_i^2 - \partial_2\omega(R_{ab}, R_{ab})\sum_{i=1}^{N}\alpha_i^2 x_i^2$$

$$= -\sum_{i=1}^{N}\alpha_i\left[\partial_1\omega(R_{ab}, R_{ab}) + \alpha_i\partial_2\omega(R_{ab}, R_{ab})\right]x_i^2.$$

By inspection, a sufficient condition for positive-definiteness is the pair of constraints

$$\partial_1\omega(R_{ab}, R_{ab}) < 0, \qquad \partial_1\omega(R_{ab}, R_{ab}) + \partial_2\omega(R_{ab}, R_{ab}) < 0.$$

These constraints are also necessary when accounting for all possible weights. From [5], these hold whenever $b \in (b^*, a)$. As such, the spherical shell with radius R_{ab} is a local minimizer of the energy function in this range and all sufficiently close convex combinations of spherical shells will converge to it. Consequently, if there is a range of parameters for which one can show that $\delta_{R_{ab}}$ is the only stationary state, then all solutions will converge toward it.

Remark 6.3. Theorem 6.1 allows us to reduce the question of global asymptotic stability of the spherical shell at R_{ab} to the clarification of uniqueness/nonuniqueness of locally stable stationary states, which is not a trivial task. One needs to find conditions for the uniqueness of local (global) minimizers of the discrete energy (6.1).

To elucidate and extend this result, let us consider the Hessian evaluated for all radii identical but an arbitrary value r. Then

$$x^T H[r]x = -\sum_{i=1}^{N}\alpha_i\left[\partial_1\omega(r, r) + \alpha_i\partial_2\omega(r, r)\right]x_i^2.$$

The convexity at radius r constraints takes the form

$$0 > \partial_1\omega(r, r) = \frac{1}{2}c(a, d)r^{b-2}\left[g(a, d)r^{a-b} - g(b, d)R_{ab}^{a-b}\right]$$

and

$$0 > (\partial_1 + \partial_2)\omega(r, r) = c(a, d)r^{b-2}\left[(a-1)r^{a-b} - (b-1)R_{ab}^{a-b}\right].$$

See (A.1) and (A.3) for the expressions for c and g, respectively. In both cases, the factor out front is negative, allowing us to reduce the constraints to

$$g(a, d)r^{a-b} > g(b, d)R_{ab}^{a-b}, \qquad (a-1)r^{a-b} > (b-1)R_{ab}^{a-b}.$$

These constraints provide a range of values along the diagonal for which the energy function is convex.

For $2 \leq d \leq 6$, the function $g(x, d) > 0$ for all $x > 3 - d$, so the energy function will always be locally convex on the diagonal for sufficiently large radii. When $d > 6$, more care is needed in characterizing the regions where this is true. These constraints extend the stability of the steady state $\delta_{R_{ab}}$ to convex combinations of spherical shells sufficiently close to a range of radii on the diagonal.

For further clarification, it is worth considering counterexamples. Consider the case $d = 3$ and $a = 2$, where $b^* = 1$. Let $b = 1.5$; then $R_{ab} = \frac{32}{49}$. From this, one can compute

$$\partial_1 \omega(r, r) = \frac{\sqrt{2}}{7\sqrt{r}} - 1, \qquad (\partial_1 + \partial_2)\omega(r, r) = \frac{2\sqrt{2}}{7\sqrt{r}} - 1,$$

so that

$$H[r] = \left(1 - \frac{\sqrt{2}}{7\sqrt{r}}\right) A + \left(1 - \frac{2\sqrt{2}}{7\sqrt{r}}\right) \alpha^T \alpha.$$

Taking the radius $r = \frac{8}{49}$ gives $H\left[\frac{8}{49}\right] = -A$, where A is a diagonal matrix with positive entries. Therefore, the energy functional is locally concave here. This helps illustrate the difficulties in determining global minimizers of the energy function.

Alternatively, taking equally weighted shells, i.e., each $\alpha_i = \frac{1}{N}$, simplifies the picture. In particular, the Hessian at a diagonal point becomes

$$H[r] = -\frac{1}{N}\partial_1\omega(r, r)I - \frac{1}{N^2}\partial_2\omega(r, r)\vec{1}\,\vec{1}^T,$$

where I denotes the identity matrix and $\vec{1}$ denotes the column vector containing 1 in each entry. This matrix is circulant and therefore diagonalizable by the Fourier transform.

Let $\mathcal{F}$ denote the standard unitary representation of the discrete Fourier transform. Then

$$\mathcal{F}H[r]\mathcal{F}^{-1} = -\frac{1}{N}\partial_1\omega(r, r)I - \frac{1}{N}\partial_2\omega(r, r)e_1 e_1^T.$$

At each radius r on the diagonal, the Hessian has eigenvalues

$$\lambda_1 = -\frac{1}{N}\left(\partial_1 + \partial_2\right)\omega(r, r), \qquad \lambda_{2,\dots,N} = -\frac{1}{N}\partial_1\omega(r, r).$$

Therefore, the previous constraints completely characterize the behavior on the diagonal and are necessary and sufficient for convexity.

7. Convergence of spherical shell steady states to continuous steady states.
As mentioned previously, one avenue worth pursuing is determining the relationship between the spherical shell solutions and those of the continuous PDE. To help shed some light on this relationship and motivate further investigation into spherical shell solutions, we turn to a particular case. Certain parameter choices simplify the evolution equations and allow steady states to be computed by hand. For example, the parameter values $d \geq 2$, $a = 2$, and $b = 2 - d$ localize the PDE which results in a corresponding decoupled ODE system.

Consider the function $\omega(r, s)$ for these parameters. The attractive component is

$$\omega_a(r, s) = -\frac{\omega_{d-1}}{\omega_d} \int_0^\pi (r - s \cos \theta) \sin^{d-2} \theta \ d\theta = -r.$$

The repulsive component is

$$\omega_b(r, s) = -\frac{\omega_{d-1}}{\omega_d} \int_0^\pi (r - s \cos \theta)(r^2 + s^2 - 2rs \cos \theta)^{-d/2} \sin^{d-2} \theta \ d\theta$$

$$= -\frac{2^{d-1} r (1 + \text{sgn}(r - s))}{(r + s + |r - s|)^d},$$

where $\text{sgn}(x)$ is the signum function

$$\text{sgn}(x) = \begin{cases} 1, & x > 0, \\ -1, & x < 0, \\ 0, & x = 0. \end{cases}$$

From this, we can compute the evolution equations for a system of N spherical shells as

$$\frac{dR_k}{dt} = \sum_{j=1}^N \alpha_j \omega(R_k, R_j) = \sum_{j=1}^N \alpha_j \left[-R_k + \frac{2^{d-1} R_k (1 + \text{sgn}(R_k - R_j))}{(R_k + R_j + |R_k - R_j|)^d} \right]$$

$$= -R_k + \sum_{j<k} \frac{\alpha_j}{R_k^{d-1}} + \frac{\alpha_k}{2R_k^{d-1}} = -R_k + \frac{\gamma_k}{R_k^{d-1}}, \qquad \gamma_k = \frac{\alpha_k}{2} + \sum_{j<k} \alpha_j,$$

for $k = 1, 2, \ldots, N$. One may easily deduce the steady state solution $\bar{R}_k = \gamma_k^{1/d}$. Indeed, the solution of this system is easily given by

$$R_k(t) = \left[\gamma_k \left(1 - e^{-dt} \right) + R_k^d(0) e^{-dt} \right]^{1/d}.$$

The continuous steady state for this case, found in [34, 33, 22], is a uniform distribution on a ball of radius 1. We attain a powerful convergence result if we assume the ratio of largest to smallest shell mass is uniformly bounded for all N. Such a hypothesis holds, for example, in the case of equiweighted shells.

Theorem 7.1. *Let $d \geq 2$, $a = 2$, and $b = 2 - d$. A sequence of steady states to the ODE system*

$$\{\bar{\rho}_N\}_{N=1}^\infty, \qquad \bar{\rho}_N(r) = \sum_{k=1}^N \alpha_{N,k} \delta_{\bar{R}_{N,k}}(r), \qquad \alpha_{N,k} \in (0, 1), \qquad \sum_{k=1}^N \alpha_{N,k} = 1,$$

converges in the ∞-Wasserstein distance to the energy minimizer if the ratio of largest to smallest spherical shell mass distribution is uniformly bounded for all N.

Proof. For the chosen parameters, the energy minimizer has the simple pseudo-inverse $\bar{\varphi}(\xi) = \xi^{1/d}$. The spherical shell steady state pseudo-inverses are

$$\bar{\varphi}_N(\xi) = \sum_{k=1}^{N} \chi_{N,k}(\xi)\gamma_{N,k}^{1/d}, \qquad \chi_{N,k}(\xi) = \chi_{(\beta_{N,k-1},\beta_{N,k})}(\xi),$$

where

$$\gamma_{N,k} = \frac{\beta_{N,k-1} + \beta_{N,k}}{2}, \quad \beta_{N,k} = \sum_{j=1}^{k} \alpha_{N,k}, \quad \beta_{N,0} = 0.$$

Consider the L^∞-distance of the pseudo-inverses

$$||\bar{\varphi}_N - \bar{\varphi}||_{L^\infty} = \sup_{0 \leq \xi \leq 1} |\bar{\varphi}_N(\xi) - \bar{\varphi}(\xi)| = \max_{k} \sup_{\beta_{N,k-1} \leq \xi \leq \beta_{N,k}} \left| \gamma_{N,k}^{1/d} - \xi^{1/d} \right|.$$

The function $\bar{\varphi}(\xi)$ is strictly increasing, and

$$\bar{\varphi}(\beta_{N,k-1}) \leq \gamma_{N,k}^{1/d} \leq \bar{\varphi}(\beta_{N,k}).$$

Thus,

$$\sup_{\beta_{N,k-1} \leq \xi \leq \beta_{N,k}} \left| \gamma_{N,k}^{1/d} - \xi^{1/d} \right| \leq \beta_{N,k}^{1/d} - \beta_{N,k-1}^{1/d} \leq C(N)\alpha_{N,k}^{1/d}.$$

To clarify the last inequality, note that $f(x) = x^{1/d}$ is a continuously differentiable function on the interval $[\beta_{N,k-1}, \beta_{N,k}]$. As a consequence,

$$\beta_{N,k}^{1/d} - \beta_{N,k-1}^{1/d} \leq \max_{x \in [\beta_{N,k-1}, \beta_{N,k}]} \frac{1}{d} x^{1/d-1}(\beta_{N,k} - \beta_{N,k-1})$$

$$= \frac{1}{d} \frac{\alpha_{N,k}}{\beta_{N,k-1}^{1-1/d}} \leq \frac{\alpha_{N,k}}{\alpha_{N,\min}^{1-1/d}} \leq C(N)\alpha_{N,k}^{1/d}, \qquad C(N) = \left(\frac{\alpha_{N,\max}}{\alpha_{N,\min}} \right)^{1-1/d}.$$

For the special case $k = 1$, it trivially holds that

$$\beta_{N,1}^{1/d} - \beta_{N,0}^{1/d} = \alpha_{N,1}^{1/d}.$$

Finally,

$$\lim_{N \to \infty} ||\bar{\varphi}_N - \bar{\varphi}||_{L^\infty} \leq \lim_{N \to \infty} \max_{k} \max\{C(N), 1\} \alpha_{N,k}^{1/d} \leq C \lim_{N \to \infty} \alpha_{N,\max}^{1/d}.$$

The last inequality follows from the assumption on the ratio of mass distributions of the shells and the fact that $f(x) = x^{1/d}$ is strictly increasing on $(0, 1)$. Since $f(x)$ is also continuous, the right-hand side vanishes in the limit. The requirement that the masses sum to unity and the ratio of largest to smallest remains bounded guarantees that all of the individual weights become arbitrarily small as $N \to \infty$. ∎

Approaching the general problem requires more sophisticated tools. Even minor changes to the parameters, such as trying $a = 4$, $b = 2 - d$, or $a = 2$ with b general, introduce enough complication to elude analytic techniques used in the previous proof. Furthermore, some care is needed when attempting to make energy arguments.

For the parameter range $b < b^*$, consider a sequence of steady states $\{\bar{\rho}_N\}_{N=1}^\infty$ where $\bar{\rho}_k$ has k spherical shells. Let $\bar{\rho}_*$ be a (potentially unique) minimizer of the energy functional. By the fattening instability condition from [5], one should be able to arrange $E[\bar{\rho}_*] \leq E[\bar{\rho}_N] \leq E[\bar{\rho}_1] = E[\delta_{R_{ab}}]$ for all $N \in \mathbb{N}$. By the Bolzano–Weierstrass property, there exists a convergent subsequence of $\{E[\bar{\rho}_N]\}_{N=1}^\infty$. Indeed, it may be arranged for the sequence $\{E[\bar{\rho}_N]\}_{N=1}^\infty$ to be monotonically decreasing and thus convergent. However, it is not clear that the sequence of steady state solutions $\{\bar{\rho}_N\}_{N=1}^\infty$ converges to a limit.

One must be careful in arranging such a sequence of equilibria for increasing numbers of shells. Numerical results suggest that increasing N may momentarily increase the entropy/interaction energy of a steady state. In Figure 3, we show energy computations in different parameter regimes for several values of N. In the case $b = .7$, the spherical shell $\delta_{R_{ab}}$ is the stable steady state. For $b = -.5$ and $b = -1.1$, the Carrillo–Huang equilibrium is the steady state. The value $b = -.1$ lies in the ambiguous parameter regime.
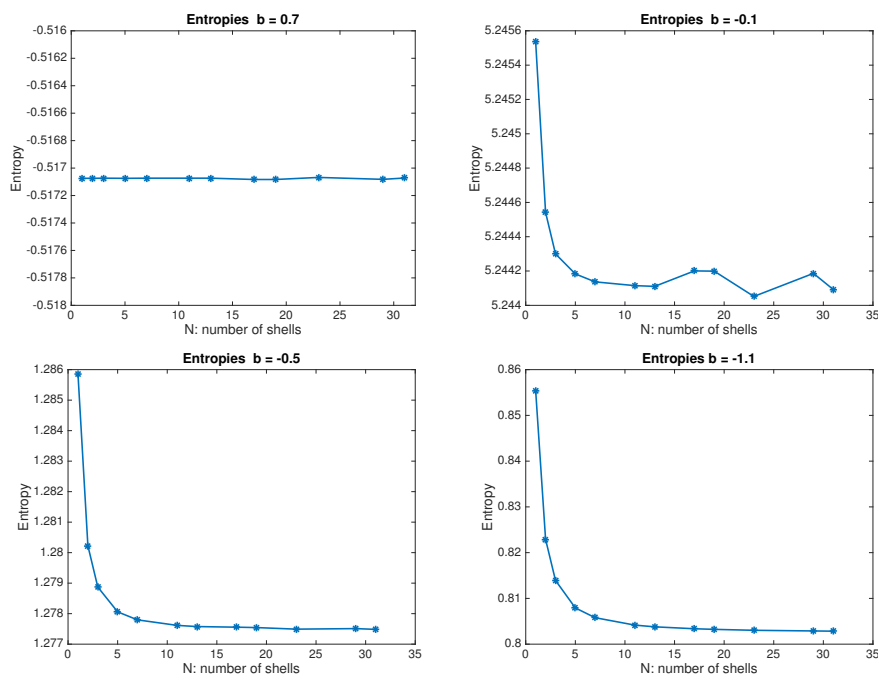

Figure 3. *Entropy/interaction energy of steady states versus number of spherical shells for $d = 3$ and $a = 4$ when $b = .7$, $-.1$, $-.5$, and -1.1.*

As the repulsive exponent moves to the region in which uniqueness is guaranteed by [44], $b \in (-d, 2 - d)$, the energy curves become more stable. Investigating the energy functional on the submanifolds spanned by larger numbers of spherical shells may help clarifying why uniqueness holds in this parameter region and whether local minimizers may exist in others.

As seen in [11] for the particle system, as the repulsive power crosses the threshold of stability for a single spherical shell, particles begin to align themselves on multiple spheres.

8. Conclusions and further research. The spherical shell framework provides an interesting new approach to exploring solutions to the radially symmetric aggregation equation in a broad functional setting. These distributional solutions exist in a kind of "world of their own" yet may have important relationships to more regular L^p solutions. The authors are currently exploring the explicit relationship between the spherical shell and continuous cases. Approaches such as those in [27, 17] using Γ-convergence of interaction energy functionals may ultimately bridge the gap.

Another aspect of this framework to be presented by the authors is the creation of a new numerical method based on the ODE system. In short, allowing the number of spherical shells to become arbitrarily large causes the ODE solutions to approximate those in the continuous case. Initial findings have been promising.

Recall that in the case for $a = 4$, the Carrillo–Huang equilibria are only guaranteed for $-d < b < \bar{b} = \frac{2 + 2d - d^2}{d + 1}$. When the repulsive power is in the region $b \in (\bar{b}, b^*)$, the proposed equilibria of the energy functional become negative near the origin. Figure 4 shows several cases of $d = 3$, $a = 4$, and correspondingly $b \in (-\frac{1}{4}, \frac{1}{2})$.
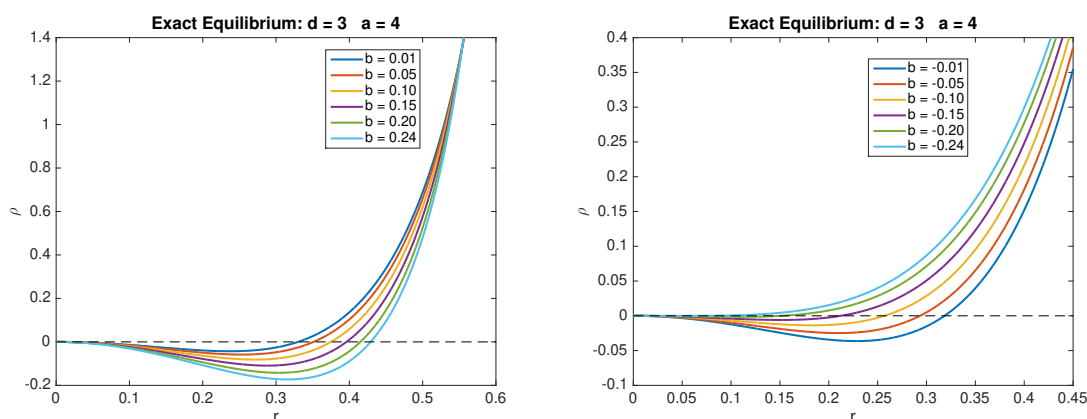

Figure 4. *Several unphysical equilibrium densities for $d = 3$ and $a = 4$.*

One advantage of the spherical shell approach is that it yields insight into the steady states within the parameter region where the Carrillo–Huang equilibria have negative regions. By allowing the number of spherical shells to approach infinity, we may be able to ascertain the true equilibria.

Appendix A. Properties of the omega function. In this section, we present some computations regarding the function ω defined in (1.3). We focus on computationally convenient forms of $\omega(r, s)$ and its derivatives in each component, especially their evaluations along the diagonal $s = r$.

For convenience, we first split ω into separate attractive and repulsive components

$$\omega(r, s) = \omega_a(r, s) - \omega_b(r, s),$$

defined by restricting the definition to the attractive (resp., repulsive) part of the potential W. By changing the surface integral from rectangular to spherical coordinates, one obtains the expression for the component terms

$$\omega_x(r,s) = -\frac{\omega_{d-1}}{\omega_d} \int_0^\pi (r - s\cos\theta)(r^2 + s^2 - 2rs\cos\theta)^{x/2-1} \sin^{d-2}\theta \, d\theta.$$

Evaluating along the diagonal simplifies the term to

$$\omega_x(r,r) = -\frac{\omega_{d-1}}{\omega_d} 2^{x/2-1} r^{x-1} \int_0^\pi (1 - \cos\theta)^{x/2-1} \sin^{d-2}\theta \, d\theta$$

$$= -2^{x+d-3} \frac{\omega_{d-1}}{\omega_d} \beta\left(\frac{x+d-1}{2}, \frac{d-1}{2}\right) r^{x-1},$$

which is well-defined for $x > 1 - d$. For simplicity, we denote the term

$$(A.1) \qquad c(x,d) = -2^{x+d-3} \frac{\omega_{d-1}}{\omega_d} \beta\left(\frac{x+d-1}{2}, \frac{d-1}{2}\right),$$

so that

$$(A.2) \qquad \omega(r,r) = c(a,d)r^{a-1} - c(b,d)r^{b-1}.$$

We remark briefly on an important relationship between quantities here. Noting that ω vanishes along the diagonal at $r = R_{ab}$ [5], where R_{ab} is still defined as in (1.5), we see that

$$0 = \omega(R_{ab}, R_{ab}) = c(a,d)R_{ab}^{a-1} - c(b,d)R_{ab}^{b-1}.$$

Simply rearranging the terms gives the equality

$$R_{ab}^{a-b} = \frac{c(b,d)}{c(a,d)}.$$

We turn to the derivatives of ω in both r and s. Working with the component terms,

$$\frac{\partial \omega_x}{\partial r}(r,s) = -\frac{\omega_{d-1}}{\omega_d} \int_0^\pi \left[(r^2 + s^2 - 2rs\cos\theta)^{x/2-1}\right.$$
$$\left. + (x-2)(r - s\cos\theta)^2(r^2 + s^2 - 2rs\cos\theta)^{x/2-2}\right] \sin^{d-2}\theta \, d\theta.$$

Evaluating along the diagonal gives

$$\partial_1 \omega_x(r,r) = -\frac{\omega_{d-1}}{\omega_d} 2^{x/2-2} r^{x-2} \int_0^\pi \left[2(1-\cos\theta)^{x/2-1} + (x-2)(1-\cos\theta)^{x/2}\right] \sin^{d-2}\theta \, d\theta$$

$$= -\frac{\omega_{d-1}}{\omega_d} 2^{x+d-4} r^{x-2} \Gamma\left(\frac{d-1}{2}\right) \left[\frac{\Gamma\left(\frac{x+d-3}{2}\right)}{\Gamma\left(\frac{x}{2}+d-2\right)} + (a-2)\frac{\Gamma\left(\frac{x+d-1}{2}\right)}{\Gamma\left(\frac{x}{2}+d-1\right)}\right]$$

$$= -\frac{\omega_{d-1}}{\omega_d} 2^{x+d-4} r^{x-2} \beta\left(\frac{x+d-1}{2}, \frac{d-1}{2}\right) \left[\frac{\frac{x}{2}+d-2}{\frac{x+d-3}{2}} + (x-2)\right]$$

$$= \frac{1}{2} c(x,d) r^{x-2} \left[\frac{x^2 + (d-4)x + 2}{x+d-3}\right],$$

which is well-defined for $x > 3 - d$. For concision, we denote

$$(A.3) \qquad g(x, d) = \frac{x^2 + (d - 4)x + 2}{x + d - 3},$$

so that

$$\partial_1 \omega(r, r) = \frac{1}{2} c(a, d) g(a, d) r^{a-2} - \frac{1}{2} c(b, d) g(b, d) r^{b-2}$$

$$= \frac{1}{2} c(a, d) r^{b-2} \left[g(a, d) r^{a-b} - g(b, d) R_{ab}^{a-b} \right].$$

Turning to the derivative with respect to s,

$$\frac{\partial \omega_x}{\partial s}(r, s) = - \frac{\omega_{d-1}}{\omega_d} \int_0^\pi \left[- \cos\theta (r^2 + s^2 - 2rs \cos\theta)^{x/2-1} \right.$$
$$\left. + (x - 2)(r - s \cos\theta)(s - r \cos\theta)(r^2 + s^2 - 2rs \cos\theta)^{x/2-2} \right] \sin^{d-2}\theta \, d\theta.$$

This derivative by itself will not end up being insightful. However, we show later that the sum of the respective derivatives along the diagonal will be. In that vein,

$$\frac{\partial \omega_x}{\partial r}(r, s) + \frac{\partial \omega_x}{\partial s}(r, s) = - \frac{\omega_{d-1}}{\omega_d} \int_0^\pi \left[(1 - \cos\theta)(r^2 + s^2 - 2rs \cos\theta)^{x/2-1} \right.$$
$$\left. + (x - 2)(r - s \cos\theta)(r + s - (r + s) \cos\theta)(r^2 + s^2 - 2rs \cos\theta)^{x/2-2} \right] \sin^{d-2}\theta \, d\theta.$$

Evaluating along the diagonal,

$$(\partial_1 + \partial_2)\omega_x(r, r) = - \frac{\omega_{d-1}}{\omega_d} 2^{x/2-1} r^{x-2} \int_0^\pi (x - 1)(1 - \cos\theta)^{x/2} \sin^{d-2}\theta \, d\theta$$

$$= - \frac{\omega_{d-1}}{\omega_d} 2^{x+d-3}(x - 1)\beta \left(\frac{x + d - 1}{2}, \frac{d - 2}{2} \right) r^{x-2}.$$

This expression is well-defined for $x > 1 - d$. Putting both components together gives

$$(\partial_1 + \partial_2)\omega(r, r) = c(a, d)(a - 1)r^{a-2} - c(b, d)(b - 1)r^{b-2}$$

$$= c(a, d) r^{b-2} \left[(a - 1)r^{a-b} - (b - 1)R_{ab}^{a-b} \right].$$

Additionally, we remark that following [5] the function ω can be expressed as

$$\omega(r, s) = r^{b-1} \psi_b \left(\frac{s}{r} \right) - r^{a-1} \psi_a \left(\frac{s}{r} \right),$$

$$\psi_x(\tau) = \frac{\omega_{d-1}}{\omega_d} \int_0^\pi (1 - \tau \cos\theta)(1 + \tau^2 - 2\tau \cos\theta)^{x/2-1} \sin^{d-2}\theta \, d\theta.$$

The properties of the function $\psi_x(\tau)$ can be found in [30, Lemma 4.4] and are summarized in the following lemma.

Lemma A.1 (properties of the function ψ_x).
- *For $x \in (2-d, 2)$, the function $\psi_x(\tau)$ is continuous, positive, and nonincreasing on $[0, \infty)$.*
- *For $x = 2$, the function $\psi_x(\tau) \equiv 1$ on $[0, \infty)$.*
- *For $x > 2$, the function $\psi_x(\tau)$ is continuous, positive, and nondecreasing on $[0, \infty)$.*

In addition, in all three situations, $\psi_x(\tau)$ satisfies

$$\psi(0) = 1 \quad and \quad \lim_{\tau \to \infty} \psi_x(\tau)\tau^{2-x} = \frac{d+x-2}{d}.$$

Appendix B. Polynomial expression for the omega function. In the case $d = 3$, the function $\omega(r, s)$ may be written in purely algebraic form. We present and deduce this form. We begin by recalling that this function may be written as

$$\omega(r, s) = \omega_a(r, s) - \omega_b(r, s),$$

where

$$\omega_a(r, s) = -\frac{\omega_{d-1}}{\omega_d} \int_0^\pi (r - s\cos\theta)(r^2 + s^2 - 2rs\cos\theta)^{a/2-1} \sin^{d-2}\theta \; d\theta.$$

When $a = 2k$, the attraction component is a polynomial of r and s. When $d = 3$, $b > -2$, and $r \neq s$, the repulsive component may be written as

$$\begin{aligned}
\omega_b(r, s) &= -\frac{1}{2} \int_0^\pi (r - s\cos\theta)(r^2 + s^2 - 2rs\cos\theta)^{b/2-1} \sin\theta \; d\theta \\
&= -\frac{1}{8r^2 s} \int_{(r-s)^2}^{(r+s)^2} (u + r^2 - s^2)u^{b/2-1} du \\
&= \frac{-(br + r - s)(r + s)^{b+1} + (r - s)(br + r + s)|r - s|^b}{2b(b+2)r^2 s}.
\end{aligned}$$

The energy functional for convex combinations of spherical shells may also be rewritten in algebraic form using similar substitutions. Noting that

$$E[\rho] = E_a[\rho] - E_b[\rho],$$

where $E_a[\rho]$ is a polynomial for even $a > 0$, the repulsive component takes the form

$$E_b[\rho] = \frac{1}{4b(b+2)} \sum_{i=1}^n \frac{\alpha_i}{R_i} \sum_{j=1}^n \frac{\alpha_j}{R_j} \left[(R_i + R_j)^{b+2} - |R_i - R_j|^{b+2} \right].$$

REFERENCES

[1] G. Albi, D. Balagué, J. A. Carrillo, and J. von Brecht, *Stability analysis of flock and mill rings for second order models in swarming*, SIAM J. Appl. Math., 74 (2014), pp. 794–818, https://doi.org/10.1137/13091779X.

[2] L. Ambrosio, N. Gigli, and G. Savaré, *Gradient Flows in Metric Spaces and in the Space of Probability Measures*, 2nd ed., Lectures Math. ETH Zürich, Birkhäuser Verlag, Basel, 2008.

[3] L. Ambrosio and S. Serfaty, *A gradient flow approach to an evolution problem arising in superconductivity*, Comm. Pure Appl. Math., 61 (2008), pp. 1495–1539, https://doi.org/10.1002/cpa.20223.

[4] D. Balagué, J. A. Carrillo, T. Laurent, and G. Raoul, *Dimensionality of local minimizers of the interaction energy*, Arch. Ration. Mech. Anal., 209 (2013), pp. 1055–1088, https://doi.org/10.1007/s00205-013-0644-6.

[5] D. Balagué, J. A. Carrillo, T. Laurent, and G. Raoul, *Nonlocal interactions by repulsive-attractive potentials: Radial ins/stability*, Phys. D, 260 (2013), pp. 5–25, https://doi.org/10.1016/j.physd.2012.10.002.

[6] D. Balagué, J. A. Carrillo, and Y. Yao, *Confinement for repulsive-attractive kernels*, Discrete Contin. Dyn. Syst. Ser. B, 19 (2014), pp. 1227–1248, https://doi.org/10.3934/dcdsb.2014.19.1227.

[7] A. Barbaro, B. Einarsson, B. Birnir, S. Sigurdsson, H. Valdimarsson, Ó. K. Pálsson, S. Sveinbjörnsson, and T. Sigurdsson, *Modelling and simulations of the migration of pelagic fish*, ICES J. Mar. Sci., 66 (2009), pp. 826–838.

[8] A. B. T. Barbaro, K. Taylor, P. F. Trethewey, L. Youseff, and B. Birnir, *Discrete and continuous models of the dynamics of pelagic fish: Application to the capelin*, Math. Comput. Simulation, 79 (2009), pp. 3397–3414, https://doi.org/10.1016/j.matcom.2008.11.018.

[9] D. Benedetto, E. Caglioti, and M. Pulvirenti, *Erratum: "A kinetic equation for granular media"* [*RAIRO Modél. Math. Anal. Numér.*, 31 (1997), *pp.* 615–641; MR1471181], M2AN Math. Model. Numer. Anal., 33 (1999), pp. 439–441, https://doi.org/10.1051/m2an:1999118.

[10] A. L. Bertozzi, J. A. Carrillo, and T. Laurent, *Blow-up in multidimensional aggregation equations with mildly singular interaction kernels*, Nonlinearity, 22 (2009), pp. 683–710, https://doi.org/10.1088/0951-7715/22/3/009.

[11] A. L. Bertozzi, T. Kolokolnikov, H. Sun, D. Uminsky, and J. von Brecht, *Ring patterns and their bifurcations in a nonlocal model of biological swarms*, Commun. Math. Sci., 13 (2015), pp. 955–985, https://doi.org/10.4310/CMS.2015.v13.n4.a6.

[12] A. L. Bertozzi, T. Laurent, and J. Rosado, L^p *theory for the multidimensional aggregation equation*, Comm. Pure Appl. Math., 64 (2011), pp. 45–83, https://doi.org/10.1002/cpa.20334.

[13] B. Birnir, *An ODE model of the motion of pelagic fish*, J. Stat. Phys., 128 (2007), pp. 535–568, https://doi.org/10.1007/s10955-007-9292-2.

[14] A. Blanchet, V. Calvez, and J. A. Carrillo, *Convergence of the mass-transport steepest descent scheme for the subcritical Patlak–Keller–Segel model*, SIAM J. Numer. Anal., 46 (2008), pp. 691–721, https://doi.org/10.1137/070683337.

[15] A. Blanchet, J. A. Carrillo, and N. Masmoudi, *Infinite time aggregation for the critical Patlak-Keller-Segel model in* $\mathbb{R}^2$, Comm. Pure Appl. Math., 61 (2008), pp. 1449–1481, https://doi.org/10.1002/cpa.20225.

[16] J. A. Cañizo, J. A. Carrillo, and F. S. Patacchini, *Existence of compactly supported global minimisers for the interaction energy*, Arch. Ration. Mech. Anal., 217 (2015), pp. 1197–1217, https://doi.org/10.1007/s00205-015-0852-3.

[17] J. A. Cañizo and F. S. Patacchini, *Discrete minimisers are close to continuum minimisers for the interaction energy*, Calc. Var. Partial Differential Equations, 57 (2018), 24, https://doi.org/10.1007/s00526-017-1289-3.

[18] J. A. Carrillo, M. Chipot, and Y. Huang, *On global minimizers of repulsive-attractive power-law interaction energies*, Philos. Trans. R. Soc. Lond. Ser. A Math. Phys. Eng. Sci., 372 (2014), 20130399, 13, https://doi.org/10.1098/rsta.2013.0399.

[19] J. A. Carrillo, M. R. D'Orsogna, and V. Panferov, *Double milling in self-propelled swarms from kinetic theory*, Kinet. Relat. Models, 2 (2009), pp. 363–378, https://doi.org/10.3934/krm.2009.2.363.

[20] J. A. Carrillo, A. Figalli, and F. S. Patacchini, *Geometry of minimizers for the interaction energy with mildly repulsive potentials*, Ann. Inst. H. Poincaré Anal. Non Linéaire, 34 (2017), pp. 1299–1308, https://doi.org/10.1016/j.anihpc.2016.10.004.

[21] J. A. Carrillo, M. Fornasier, G. Toscani, and F. Vecil, *Particle, kinetic, and hydrodynamic models of swarming*, in Mathematical Modeling of Collective Behavior in Socio-economic and Life Sciences, Model. Simul. Sci. Eng. Technol., Birkhäuser Boston, Boston, MA, 2010, pp. 297–336, https://doi.org/10.1007/978-0-8176-4946-3_12.

[22] J. A. Carrillo and Y. Huang, *Explicit equilibrium solutions for the aggregation equation with power-law*

potentials, Kinet. Relat. Models, 10 (2017), pp. 171–192, https://doi.org/10.3934/krm.2017007.

[23] J. A. Carrillo, R. J. McCann, and C. Villani, *Kinetic equilibration rates for granular media and related equations: Entropy dissipation and mass transportation estimates*, Rev. Mat. Iberoamericana, 19 (2003), pp. 971–1018, https://doi.org/10.4171/RMI/376.

[24] J. A. Carrillo, R. J. McCann, and C. Villani, *Contractions in the 2-Wasserstein length space and thermalization of granular media*, Arch. Ration. Mech. Anal., 179 (2006), pp. 217–263, https://doi.org/10.1007/s00205-005-0386-1.

[25] J. A. Carrillo and J. S. Moll, *Numerical simulation of diffusive and aggregation phenomena in nonlinear continuity equations by evolving diffeomorphisms*, SIAM J. Sci. Comput., 31 (2009), pp. 4305–4329, https://doi.org/10.1137/080739574.

[26] K. Craig and A. L. Bertozzi, *A blob method for the aggregation equation*, Math. Comp., 85 (2016), pp. 1681–1717, https://doi.org/10.1090/mcom3033.

[27] K. Craig and I. Topaloglu, *Convergence of regularized nonlocal interaction energies*, SIAM J. Math. Anal., 48 (2016), pp. 34–60, https://doi.org/10.1137/15M1013882.

[28] P. Degond and S. Motsch, *Continuum limit of self-driven particles with orientation interaction*, Math. Models Methods Appl. Sci., 18 (2008), pp. 1193–1215, https://doi.org/10.1142/S0218202508003005.

[29] J. Dolbeault and B. Perthame, *Optimal critical mass in the two-dimensional Keller-Segel model in $\mathbb{R}^2$*, C. R. Math. Acad. Sci. Paris, 339 (2004), pp. 611–616, https://doi.org/10.1016/j.crma.2004.08.011.

[30] H. Dong, *The aggregation equation with power-law kernels: Ill-posedness, mass concentration and similarity solutions*, Comm. Math. Phys., 304 (2011), pp. 649–664, https://doi.org/10.1007/s00220-011-1237-6.

[31] Q. Du and P. Zhang, *Existence of weak solutions to some vortex density models*, SIAM J. Math. Anal., 34 (2003), pp. 1279–1299, https://doi.org/10.1137/S0036141002408009.

[32] K. Fellner and G. Raoul, *Stable stationary states of non-local interaction equations*, Math. Models Methods Appl. Sci., 20 (2010), pp. 2267–2291, https://doi.org/10.1142/S0218202510004921.

[33] R. C. Fetecau and Y. Huang, *Equilibria of biological aggregations with nonlocal repulsive-attractive interactions*, Phys. D, 260 (2013), pp. 49–64, https://doi.org/10.1016/j.physd.2012.11.004.

[34] R. C. Fetecau, Y. Huang, and T. Kolokolnikov, *Swarm dynamics and equilibria for a nonlocal aggregation model*, Nonlinearity, 24 (2011), pp. 2681–2716, https://doi.org/10.1088/0951-7715/24/10/002.

[35] J. Garnier, G. Papanicolaou, and T.-W. Yang, *Large deviations for a mean field model of systemic risk*, SIAM J. Financial Math., 4 (2013), pp. 151–184, https://doi.org/10.1137/12087387X.

[36] L. Gosse and G. Toscani, *Lagrangian numerical approximations to one-dimensional convolution-diffusion equations*, SIAM J. Sci. Comput., 28 (2006), pp. 1203–1227, https://doi.org/10.1137/050628015.

[37] S.-Y. Ha and E. Tadmor, *From particle to kinetic and hydrodynamic descriptions of flocking*, Kinet. Relat. Models, 1 (2008), pp. 415–435, https://doi.org/10.3934/krm.2008.1.415.

[38] R. Hegselmann and U. Krause, *Opinion dynamics and bounded confidence: Models, analysis and simulation*, J. Artif. Soc. Soc. Simul., 5 (2002).

[39] D. D. Holm and V. Putkaradze, *Formation of clumps and patches in self-aggregation of finite-size particles*, Phys. D, 220 (2006), pp. 183–196, https://doi.org/10.1016/j.physd.2006.07.010.

[40] T. Kolokolnikov, J. A. Carrillo, A. Bertozzi, R. Fetecau, and M. Lewis, *Emergent behaviour in multi-particle systems with non-local interactions [Editorial]*, Phys. D, 260 (2013), pp. 1–4, https://doi.org/10.1016/j.physd.2013.06.011.

[41] H. Li and G. Toscani, *Long-time asymptotics of kinetic models of granular flows*, Arch. Ration. Mech. Anal., 172 (2004), pp. 407–428, https://doi.org/10.1007/s00205-004-0307-8.

[42] T. Lim and R. J. McCann, *Isodiametry, Variance, and Regular Simplices from Particle Interactions*, preprint, https://arxiv.org/abs/1907.13593, 2019.

[43] F. Lin and P. Zhang, *On the hydrodynamic limit of Ginzburg-Landau vortices*, Discrete Contin. Dynam. Systems, 6 (2000), pp. 121–142, https://doi.org/10.3934/dcds.2000.6.121.

[44] O. Lopes, *Uniqueness and radial symmetry of minimizers for a nonlocal variational problem*, Commun. Pure Appl. Anal., 18 (2019), pp. 2265–2282, https://doi.org/10.3934/cpaa.2019102.

[45] E. Mainini, *A global uniqueness result for an evolution problem arising in superconductivity*, Boll. Unione Mat. Ital. (9), 2 (2009), pp. 509–528.

[46] N. MASMOUDI AND P. ZHANG, *Global solutions to vortex density equations arising from sup-conductivity*, Ann. Inst. H. Poincaré Anal. Non Linéaire, 22 (2005), pp. 441–458, https://doi.org/10.1016/j.anihpc.2004.07.002.

[47] A. MOGILNER AND L. EDELSTEIN-KESHET, *A non-local model for a swarm*, J. Math. Biol., 38 (1999), pp. 534–570, https://doi.org/10.1007/s002850050158.

[48] S. MOTSCH AND E. TADMOR, *A new model for self-organized dynamics and its flocking behavior*, J. Stat. Phys., 144 (2011), pp. 923–947, https://doi.org/10.1007/s10955-011-0285-9.

[49] S. MOTSCH AND E. TADMOR, *Heterophilious dynamics enhances consensus*, SIAM Rev., 56 (2014), pp. 577–621, https://doi.org/10.1137/120901866.

[50] E. SANDIER AND S. SERFATY, *A rigorous derivation of a free-boundary problem arising in superconductivity*, Ann. Sci. École Norm. Sup. (4), 33 (2000), pp. 561–592, https://doi.org/10.1016/S0012-9593(00)00122-1.

[51] E. SANDIER AND S. SERFATY, *Vortices in the Magnetic Ginzburg-Landau Model*, Progr. Nonlinear Differential Equations Appl. 70, Birkhäuser Boston, Boston, MA, 2007.

[52] C. M. TOPAZ, A. J. BERNOFF, S. LOGAN, AND W. TOOLSON, *A model for rolling swarms of locusts*, Eur. Phys. J. Spec. Top., 157 (2008), pp. 93–109.

[53] C. M. TOPAZ AND A. L. BERTOZZI, *Swarming patterns in a two-dimensional kinematic model for biological groups*, SIAM J. Appl. Math., 65 (2004), pp. 152–174, https://doi.org/10.1137/S0036139903437424.

[54] C. M. TOPAZ, A. L. BERTOZZI, AND M. A. LEWIS, *A nonlocal continuum model for biological aggregation*, Bull. Math. Biol., 68 (2006), pp. 1601–1623, https://doi.org/10.1007/s11538-006-9088-6.

[55] G. TOSCANI, *One-dimensional kinetic models of granular flows*, M2AN Math. Model. Numer. Anal., 34 (2000), pp. 1277–1291, https://doi.org/10.1051/m2an:2000127.

[56] C. VILLANI, *Topics in Optimal Transportation*, Grad. Stud. Math. 58, American Mathematical Society, Providence, RI, 2003, https://doi.org/10.1090/gsm/058.

[57] E. WEINAN, *Dynamics of vortex liquids in Ginzburg-Landau theories with applications to superconductivity*, Phys. Rev. B, 50 (1994), pp. 1126–1135.

[58] S. WIGGINS, *Introduction to Applied Nonlinear Dynamical Systems*, 2nd ed., Texts Appl. Math. 2, Springer, New York, 2003.